Electronic Supplementary Material (ESI) for Analytical Methods.


Supporting information for

# Trapping Chlorine Radicals via Substituting Nitro Radicals in the Gas Phase

Akira Seto, Yuki Ochi, Hiroaki Gotoh, Kazuhisa Sakakibara*, Shota Hatazawa, Kanekazu Seki, Naoaki Saito, and Yuji Mishima

Table of Contents

| | |
|---|---|
| | Figure S8. IA-QMS spectrometer: IA-Lab by Canon ANELVA. |

**Experimental Section**

**General remarks**

Mass spectral (MS) analyses were carried out using a Shimadzu Axima-CFR. Ion attachment ionization-quadrupole mass spectrometry (IA-QMS) analyses were carried out on a Canon ANELVA IA-Lab using a soft ionization technique through Li atom attachment. High-resolution mass spectral analysis (HRMS) was carried out using a Bruker Autoflex speed [standard sample: polyethylene glycol (AMW300); cationization agent: sodium trifluoroacetate; matrix: 5,10,15,20-tetrakis(pentafluorophenyl)porphyrin]. Liquid chromatography-mass spectroscopy (LC-MS) analyses were performed using a Shimadzu LCMS-2010. FT-IR spectra were recorded on a Nicolet iS10 Fourier transform infrared spectrophotometer (FT-IR) spectrometer (KBr pellet method). $^{1}$H and $^{13}$C spectra were recorded on a Bruker DRX-300, JEOL ECX-400, or Bruker DRX-500. $^{1}$H NMR data are reported in terms of chemical shift (δ ppm), peak multiplicity (s = singlet, d = doublet, t = triplet, q = quartet, m = multiplet), coupling constant (Hz), relative integration value, and assignment. $^{13}$C NMR data are reported in terms of chemical shift. Electron spin resonance (ESR) spectra were recorded on a JEOL ME-3X.

**Preparation of DPPH-Cl paramagnetic adduct ([DPPH+Cl-$NO_2$]·) and its reduced diamagnetic DPPHH-Cl adduct (DPPHH+Cl-$NO_2$) via an organic reaction in the liquid phase**

A schematic of the synthesis of the DPPH-Cl paramagnetic adduct ([DPPH+Cl-$NO_2$]·) and its reduced diamagnetic adduct DPPHH-Cl (DPPHH+Cl-$NO_2$) is shown in Scheme S1.

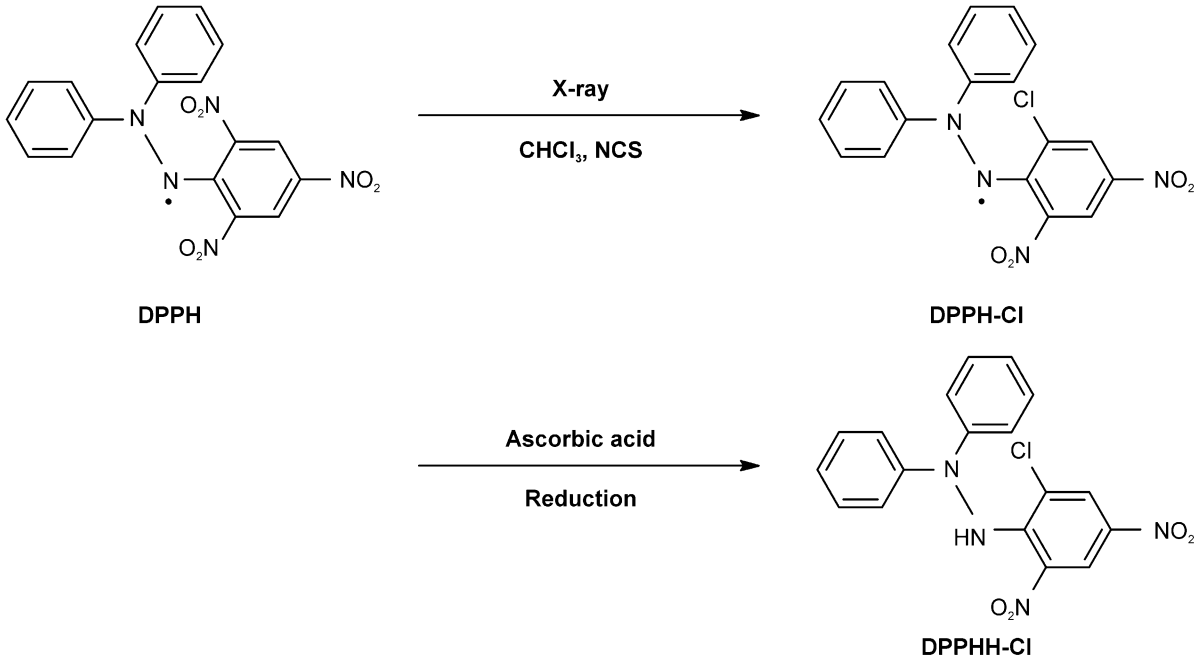


Scheme S1. Preparation of DPPH-Cl ([DPPH+Cl-$NO_2$]·) and DPPHH-Cl (DPPHH+Cl-$NO_2$).

In order to characterize the reaction product, we isolated the reaction product (DPPHH+Cl-$NO_2$) from the liquid phase experiments after reduction by ascorbic acid. By $^1$H-NMR and MS analyses of the reduced reaction product, the product was identified as DPPHH-Cl (DPPHH+Cl-$NO_2$), where the *ortho*-$NO_2$ group in the picryl ring was substituted with Cl; the yield was determined using the $^1$H-NMR integration values of the corresponding peaks. As the reaction between DPPH· and Cl· was clarified to proceed via a substitution-trapping mechanism in the liquid phase, we also carried out the same characterization process for the reaction product of DPPH· with Cl· in the gas phase. The reaction product DPPH-Cl ([DPPH+Cl-$NO_2$]·) in the gas phase was isolated and purified by preparative thin layer chromatography (TLC) using a 9:1 mixture of carbon tetrachloride/acetonitrile as the eluent; the product was characterized by ESR, IR, MS, and $^1$H-NMR. The yield of the isolated paramagnetic adduct was determined from the isolated amount of DPPH-Cl. The values of the DPPH-Cl paramagnetic adduct ([DPPH+Cl-$NO_2$]·) from the isolated amount of the adduct or as determined from the $^1$H-NMR integration

values of the reduced reaction adduct DPPHH-Cl were nearly identical.

*Preparation of DPPH-Cl ([DPPH+Cl-$NO_2$]·) in the liquid phase*

2,2-Diphenyl-1-picrylhydrazyl (DPPH) (31.8 mg, 0.0804 mmol) and *N*-chlorosuccinimide (107.6 mg, 0.806 mmol) were dissolved in $CHCl_3$. This solution was irradiated by soft X-ray using a SOFTEX SE-5005 (2 Gy/min) for 11 h. The reaction products were isolated by preparative TLC using a 9:1 mixture of carbon tetrachloride/acetonitrile as the eluent; the products were characterized by LC-MS and ESR. The yield of the DPPH-Cl paramagnetic adduct ([DPPH+Cl-$NO_2$]·) was determined from the isolated amount of the adduct.

Table S1. High-resolution mass spectrometric analysis of DPPH-Cl adduct with MALDI/TOF/MS-type Autoflex Speed equipment.

| MALDI/TOF/MS-Type Autoflex Speed | | | |
|---|---|---|---|
| Formula | Calculated exact mass | Measured m/z | Err [ppm] |
| $C_{18}H_{12}ClN_4O_4$ | 383.054160 | 383.053901 | 0.7 |

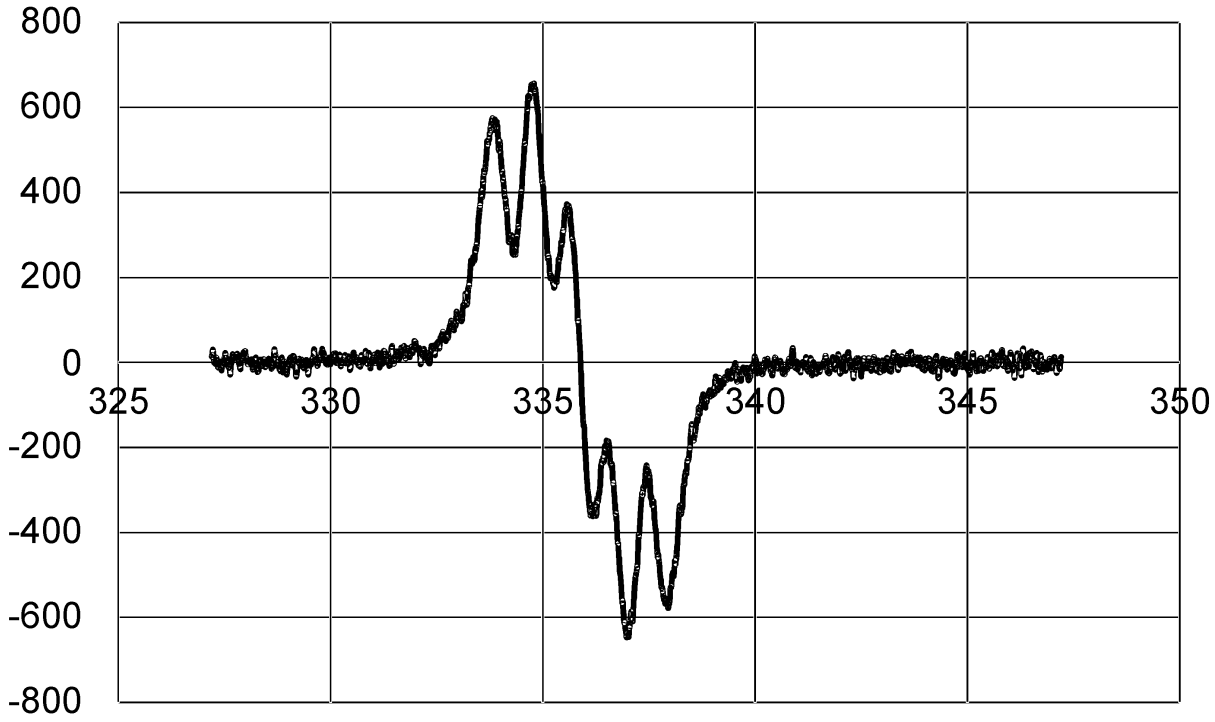


Figure S1. ESR spectrum of paramagnetic DPPH-Cl adduct ([DPPH+Cl-$NO_2$]·). Frequency = 9433 [MHz]; modulation: Fq = 100.0 kHz; width = 0.6 mT; power = 4.000 mW; sweep time = 1.0 min; time constant = 0.03 s; amplitude = 2.000.

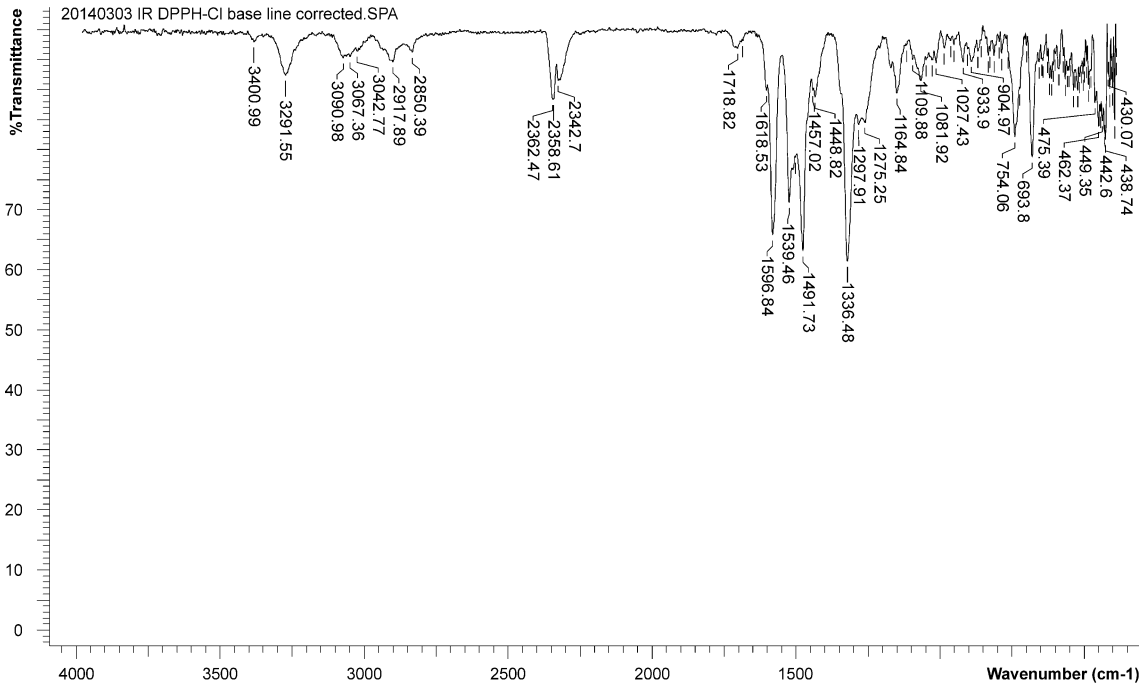


Figure S2. IR spectrum of paramagnetic DPPH-Cl adduct ([DPPH+Cl-$NO_2$]·) (KBr pellet).

*Preparation of DPPHH-Cl (DPPHH+Cl-$NO_2$) from DPPH-Cl ([DPPH+Cl-$NO_2$]·)*

A solution of the crude DPPH-Cl paramagnetic adduct in $CH_3CN$ (20 mL) was treated with a solution of ascorbic acid (142 mg, 0.8 mmol) in $H_2O$ (30 mL). After stirring the reaction mixture at ambient temperature for 5 min, the color of the solution changed from purple to yellow. The organic materials were extracted with ethyl acetate (WAKO Chemical, Extra pure grade: purity 99.0 %) (15 mL) repeatedly. The reduced diamagnetic adduct DPPHH-Cl (Rf = 0.66) was isolated by preparative TLC using a 9:1 mixture of carbon tetrachloride/acetonitrile as the eluent. The amount of DPPHH-Cl ([DPPHH+Cl-$NO_2$] obtained was 2.6 mg ($6.8\times10^{-3}$ mmol).

$^1$H NMR (300 MHz, $CDCl_3$) δ = 8.86 (2H, d, *J* = 8.6 Hz), 7.57–7.22 (11H, m), 5.51 (1H, bs), 1.29 (9H, s); $^{13}$C NMR(125 MHz, $CDCl_3$) δ = 140.0, 139.2, 136.4, 131.3, 131.0, 130.6, 129.4, 128.2, 127.2, 126.8, 124.6, 123.9, 62.2, 28.0; IR (KBr pellet) ν; 3528, 2975, 1675, 1374, 1358, 1202, 1030, 764, 426, 406 $cm^{-1}$.

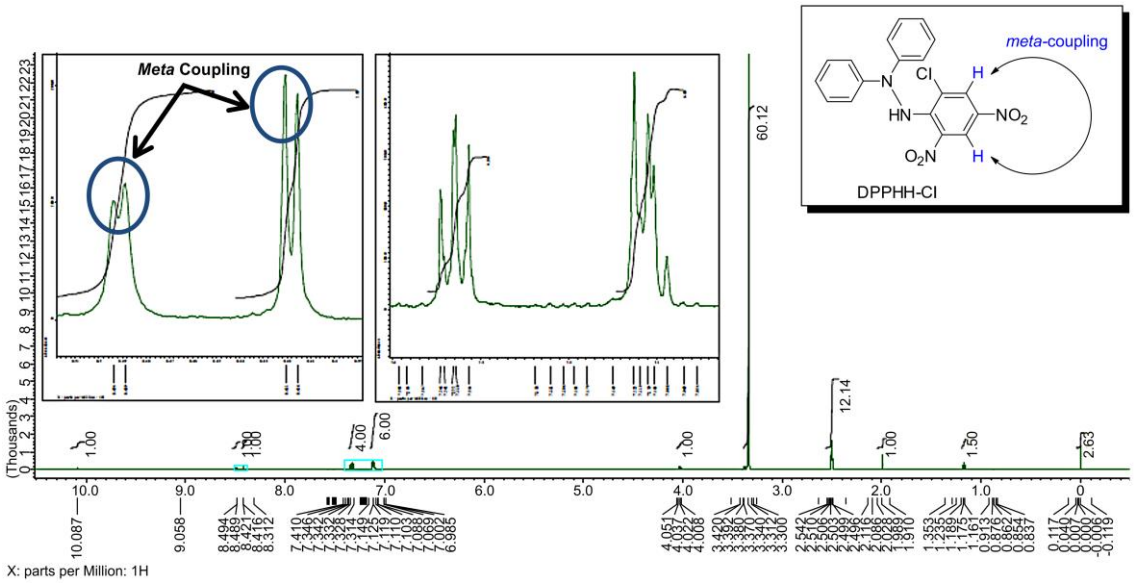


Figure S3. $^{1}$H-NMR spectrum of diamagnetic DPPHH-Cl adduct in DMSO-$d_6$ (δ in ppm) δ = 10.09 (s, 1H), 8.49 (d, J = 2.5 Hz, 1H), 8.42 (d, J = 2.5 Hz, 1H), 7.35-7.31 (m, 4H), 7.13-7.09 (m, 6H). * Peaks ascribed to ethyl acetate (used as an extraction solvent for the isolation of DPPH-Cl adduct) are recognized in the higher field region (δ: 1.0–4.1 ppm). Observed *meta*-coupling between unisochronous protons shown in Figure S3 supports that the structure of the DPPHH-Cl adduct is the one shown in the structure to the right.

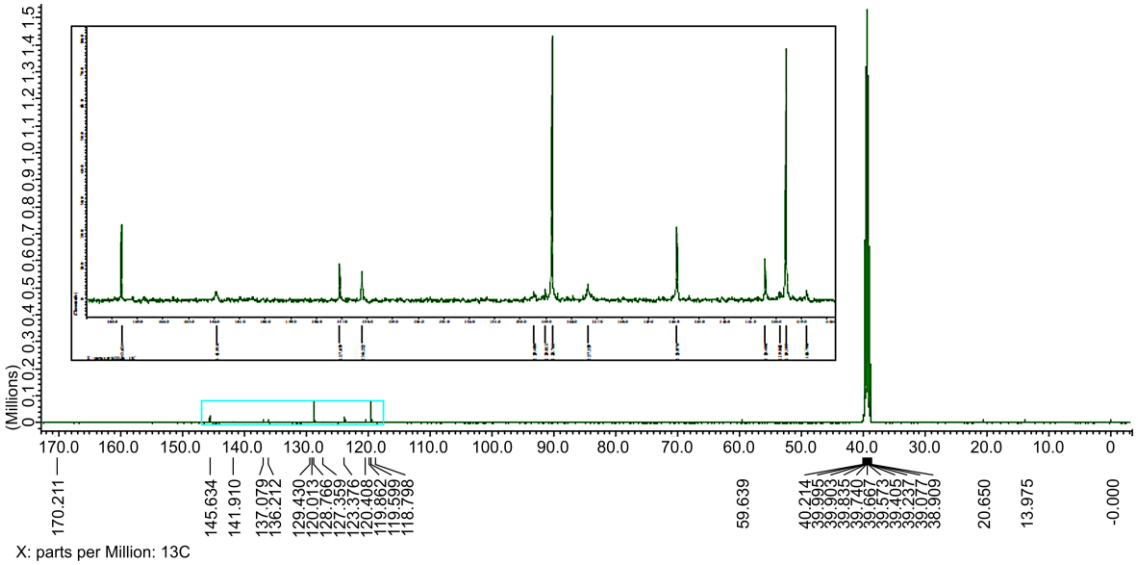


Figure S4. $^{13}$C-NMR spectrum of diamagnetic DPPHH-Cl (DPPHH+Cl-$NO_2$) adduct in DMSO-$d_6$ (δ in ppm). δ = 145.6, 141.9, 137.1, 136.2, 128.8, 127.4, 123.9, 120.4, 119.6, 118.8.

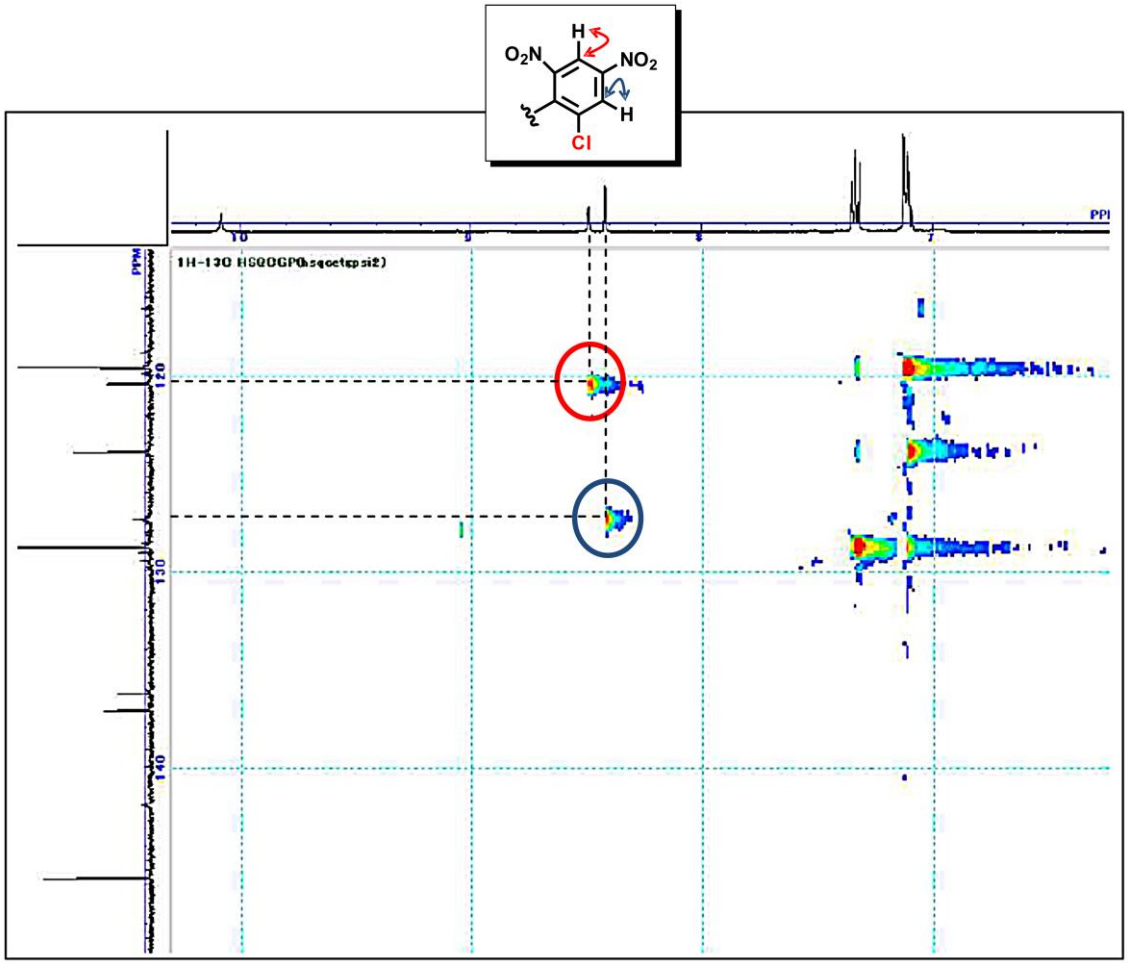


Figure S5. Two-dimensional HMQC spectrum of DPPHH-Cl adduct (DPPHH+Cl-$NO_2$) in DMSO-$d_6$ obtained on a Bruker DRX-500. $^{1}$H-NMR chemical shift is shown on the abscissa axis. $^{13}$C-NMR chemical shift is shown through the axis of the ordinate. One-bond C-H couplings, shown in the structure to the left (double-headed curled arrows), could be recognized in the two-dimensional HMQC spectrum by cross-peaks.

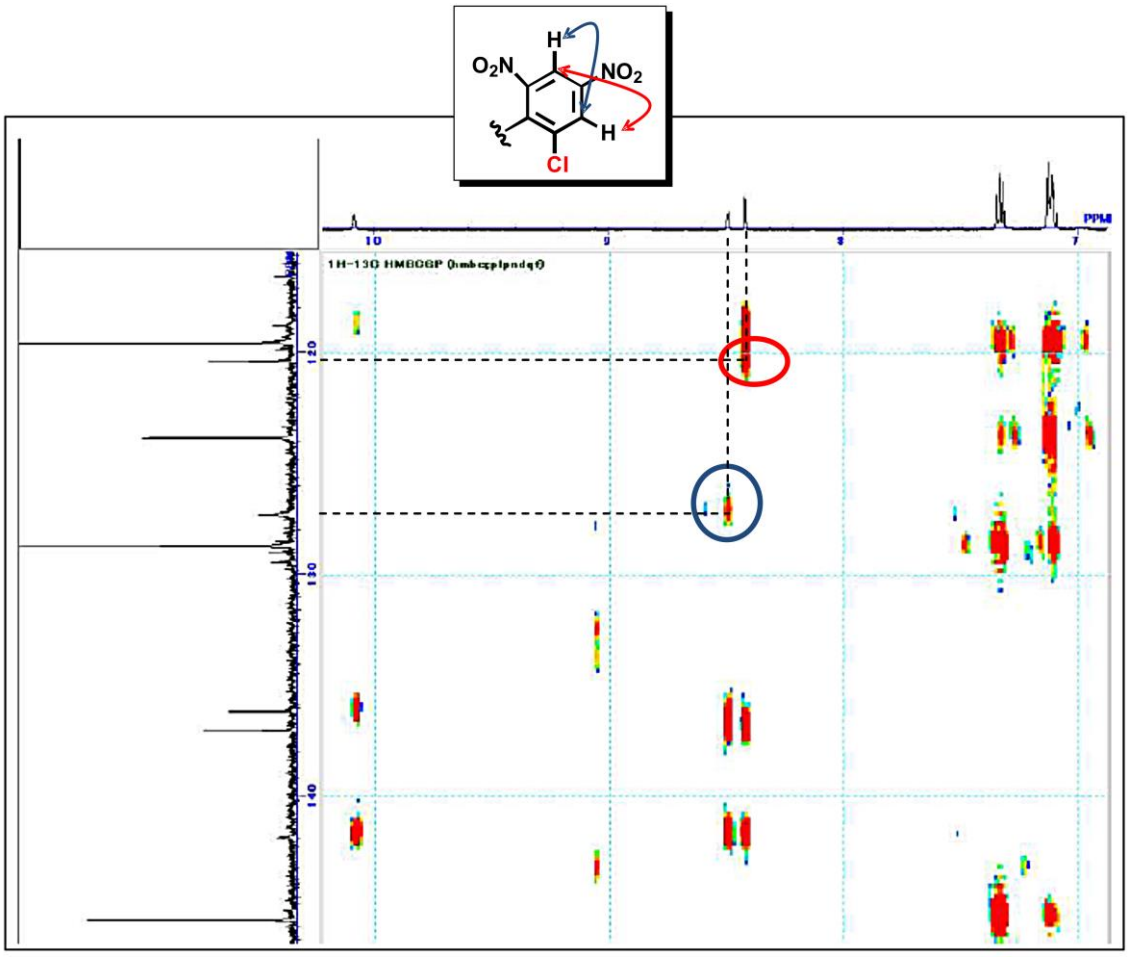


Figure S6. Two-dimensional HMBC spectrum of DPPH-Cl adduct (DPPHH+Cl-$NO_2$) conducted in DMSO-$d_6$ using a Bruker DRX-500. $^{1}$H-NMR chemical shift is shown on the abscissa axis. $^{13}$C-NMR chemical shift is shown through the axis of the ordinate. Long-range, two-bond C-H couplings, shown in the structure to the left (double-headed curled arrows), could be recognized in the two-dimensional HMBC spectrum by cross-peaks.

**Procedure for Cl· radical capture by DPPH· in the gas-phase and characterization of the DPPH-Cl paramagnetic adduct ([DPPH+Cl-$NO_2$]·)**

Cl• capture by DPPH• in the gas phase was carried out in the quartz reaction cell (cylindrical vessel with volume of 129 $cm^3$, laser path length 9 cm) shown below. The Cl• capturing square silica filter paper was set in this sample cell filled with $Cl_2$ gas (1 Torr vapor pressure). On this 3-mm-edge filter paper, DPPH• (2.6 mg/$cm^2$) was coated uniformly via application of the DPPH• solution in $CH_2Cl_2$. Cl• radicals were generated by YAG laser irradiation ($\lambda$ = 355 nm, 3.2 mJ/shot). The cross-section for $Cl_2$ absorption at $\lambda$ = 355 nm using the reaction cell was determined experimentally to be $\sigma = 1.6 \times 10^{-19}$ $cm^2$ $molecule^{-1}$. After 1 h of irradiation (10 shots in 1 s), Cl• radical-exposed silica filter paper was removed from the reaction cell and the reaction product was extracted with ethyl acetate for subsequent analysis. The yields of the DPPH-Cl paramagnetic adduct ([DPPH+Cl-$NO_2$]·) were determined using the $^1$H-NMR integration values of the reduced DPPHH-Cl reaction adduct. For the IA-QMS experiments, Cl• radical-exposed silica filter paper was placed directly in the IA-QMS ionization chamber.


Figure S7. Overview of the reaction apparatus for Cl• capturing experiments by DPPH• in the gas phase.

*Experimental procedure to evaluate the yield of DPPH-Cl adduct ([DPPH+Cl-$NO_2$]·) by IA-QMS measurements*

Soft ionization was carried out by attaching $Li^+$ ions on the IA-Lab IA-QMS equipment by Canon ANELVA. In many soft-ionization MS methods, Ion Attachment ionization (IA) -MS is assumed to be the most appropriate one because of the lack of dissociative ionization. Lithium ions ($Li^+$) attach to chemical species (M) and form adduct ions of the type $(M+Li)^+$. By taking advantage of fragment-free ionization and higher ionization efficiency, intact samples of reactive radicals as well as stable molecules can easily be observed without separation or derivation pre-treatment for characterization and quantitative analyses. An IA-quadrupole MS analyzer (IA-QMS) was employed in these studies. Chemical species on the sample silica filter paper were extracted by using a direct inlet probe with a heater and the mass was subsequently analyzed. Because the chance of fragmentation and side reactions is very small, the approximate yield can be determined directly from the ratio of the amount of the ion currents of the product and starting material in the mass-chromatogram. Thus, quantitative *in situ* sample analyses are possible. First, the appropriate temperature ranges where DPPH• and DPPH-Cl• radical adducts were ionized were explored by temperature-dependent IA-QMS experiments. By monitoring the ion current (IC) of [DPPH•]+Li (m/z: 401) and [DPPH-Cl•]+Li (m/z: 390, 392) upon increasing the chamber temperature from 30 °C to 400 °C with a temperature gradient of 64 °C $min^{-1}$, the optimum temperature ranges were determined to be [DPPH•]+Li (m/z: 401): 122–220 °C and [DPPH-Cl•]+Li (m/z: 390, 392): 114–207 °C. The amounts of [DPPH•]+Li and [DPPH-Cl•]+Li were evaluated from the observed ICs of the corresponding parent peaks and the intrinsic values of the isotope distribution patterns of the designated molecular formula (for example, [DPPH•]+Li; $C_{18}H_{12}N_5O_6Li$, the percentage of m/z: 401 against the total amount of $C_{18}H_{12}N_5O_6Li$ species is 74.88%).

Figure S8. IA-QMS spectrometer: IA-Lab by Canon ANELVA.